RAP Conference Proceedings, vol. 4, pp. 156–161, 2019
ISSN 2466-4626 (online) | doi: 10.37392/RapProc.2019.32
WWW.RAP-PROCEEDINGS.ORG

Co-60 GAMMA RADIATION INFLUENCES ON THE ELECTROCHEMICAL, PHYSICAL AND ELECTRICAL CHARACTERISTICS OF RARE-EARTH DYSPROSIUM OXIDE (Dy_2O_3)

Umutcan Gürer[1,2], Ercan Yilmaz[1,2*]

[1]Nuclear Radiation Detectors Research and Applications Center, BAIBU, Bolu, Turkey
[2]Physics Department, Bolu Abant Izzet Baysal University, Bolu, Turkey

Abstract. *In this study, the effects of gamma irradiation on the physical, electrochemical, and electrical properties of Dy_2O_3/p-Si thin films have been studied. For this, the rare earth oxide (Dy_2O_3) was deposited onto p-Si wafer by using an e-beam evaporation technique. The evolutions on the crystallographic and morphologic characteristics of the films under gamma irradiation were analyzed by X-ray diffraction (XRD) and Atomic Force Microscopy (AFM), respectively, while irradiation effects on the electrochemistry of the films were characterized by X-ray photoelectron spectroscopy (XPS). Furthermore, variations on the electrical characteristics of Dy_2O_3/p-Si thin films were also specified by Capacitance-Voltage (C-V) and Conductance-Voltage (G/ω-V) measurements. No significant changes on the crystallographic orientation were observed after gamma irradiation exposures. However, the grain size of the films was increased slightly due to the fact that the local heating aggregated the smaller grains into a bigger cluster. In addition, the surface roughness was increased after irradiation indicating that it deforms the films' surface morphology. Two different intense intermixing phases revealed the presence of the electrochemical analysis of the virgin Dy_2O_3/p-Si thin films. These phases are Dysprosium sub-Oxide (Dy_xO_y) and Oxygen deficient in Dy_2O_3 films. After irradiation exposures, Oxygen incorporation, vacancy, and interstitial defects formation were observed in the electrochemical characteristics of the films. On the other hand, the capacitance curves exhibit kinks in the region between depletion and accumulation due to the presence of the intermixing phases of Dy_2O_3 films. The capacitance of samples significantly increased with the increase of radiation doses, which are correlated with the generated interface state density and/or improvement of dielectric characteristics of Dy_2O_3 owing to Oxygen diffusion.*

Keywords: *MOS Capacitor, high-k dielectric, rare earth oxide, Dy_2O_3, irradiation*

1. INTRODUCTION

Metal-oxide-semiconductor (MOS) devices have become a crucial base of modern microelectronics technology since their discovery. Continuous developments of the MOS based technology are still focusing on the improvement of device performance. In this aspect, researchers exhibit great efforts to replace the conventional insulating SiO_2 layer with suitable high-k dielectric materials in the MOS transistor applications. High leakage current and unfavorable SiO_x and/or silicate phases are the major issues for the usage of the high-k dielectric materials in gate dielectric applications [1]–[4]. Therefore, Rare Earth Oxides (REOs) gained a lot of attention for the improvement of the MOS devices [5]–[8]. Various REOs such as Yb_2O_3 [9], Gd_2O_3 [10], [11], Sm_2O_3 [12], Y_2O_3 [13] have been reported. As a possible replacement for gate dielectrics, Dy_2O_3 is one of the most promising REO materials owing to its high dielectric constant (k = 14-18), a large energy band gap (4.9 eV), and thermal and chemical stability with silicon [14]–[16]. Researchers have already reported that Dy_2O_3 exhibits promising performance in gate dielectric applications [5], [17], [18]. However, together with these initial studies, the stability of the device should be investigated in various environments including the irradiation field to test the device reliability. To the best of our knowledge, the device characteristics under the irradiation exposure have not been investigated in great detail for the devices having the Dy_2O_3 gate dielectric. In this study, Dy_2O_3 was deposited on the p-Si substrate by the electron beam deposition (e-beam) technique to investigate the effect of Co-60 gamma radiation on the Dy_2O_3 device. The devices were exposed to Co-60 gamma irradiation up to 4000 Gy. The structural and morphological evolutions after gamma irradiation exposures were determined with X-Ray Diffraction (XRD) and Atomic Force Microscopy (AFM), respectively. The variations in the electrochemical structure of the Dy_2O_3/Si stack were investigated by X-ray photoelectron spectroscopy (XPS). The electrical characteristics of the device, capacitance-voltage (C-V) and conductance-voltage (G/ω-V) measurements were carried out.

2. EXPERIMENTAL DETAILS

The Dy_2O_3 thin films were fabricated on a p-type silicon (100) following a standard RCA (Radio Corporation of America) cleaning process. The

* yilmaz@ibu.edu.tr

substrates were immediately loaded into the e-beam chamber to avoid the environmental impurities. The substrate temperature was set to 250 °C after the base pressure of the chamber was 5x10^{-4} Pascal. The Dy_2O_3 target materials' purity was 4N and the particle size was 1-3 mm. The deposition rates were kept almost constant at 5 Å/s by controlling them with Inficon crystal sensors. The thickness of the deposited Dy_2O_3 layer was determined to be approximately 40 nm with the help of a spectroscopic reflectometer. After the deposition of the Dy_2O_3 dielectric layer, thin films were annealed in N_2 at 400 °C for one hour at an atmospheric pressure. One of the annealed wafers was cut into six pieces and MOS capacitors were fabricated by aluminum (Al) sputtering onto three thin films samples using a shadow mask with 1.5 mm diameter circular dots. Also, the back ohmic contacts were coated with Al. The Dy_2O_3 thin films were divided into three sets including one thin film and one MOS capacitors. While the first set was separated as virgin, the other sets were irradiated with Co-60 gamma irradiation. The second and third set samples were exposed to Co-60 gamma irradiation with a 417 Gy/h dose rate in the SANAEM, TAEK- Ankara, Turkey. The second group samples were exposed to 1000 Gy, while the third group samples were exposed to 4000 Gy. The film crystallography evaluations were determined by X-ray Diffraction (XRD) analyses, while atomic force microscopy (AFM) was used to investigate the surface morphological changes. X-ray photoelectron spectroscopy (XPS) measurements was employed to determine the electrochemical characteristics of Dy_2O_3/Si after etching 10 nm of the Dy_2O_3 layer with Ar sputtering before performing the XPS measurements since irradiation degradation become more visible in the deeper level of the oxide layer [19]. In addition, the irradiation-induced electrical characterizations were carried out by analyzing the series resistance corrected C-V and G/ω-V characteristics of $Al/Dy_2O_3/p\text{-}Si/Al$ MOS capacitors at 100 kHz.

3. Results and discussion

3.1. Irradiation-induced changes on the crystallographic and morphological characteristics Dy_2O_3/Si thin films

The Dy2O3 thin films' crystalline structure evolutions were determined by the XRD measurements (Fig. 1). As seen in Figure 1, the XRD patterns of the fabricated samples ordered poorly along the (222) orientation. Similar poor crystalline film structure has been previously reported for virgin Dy_2O_3 thin films annealed at 400 °C [14]. On the other hand, no significant evolution on the film crystallinity, e.g., the rise in the minor peaks' intensities or formation of secondary phases, has been observed. However, the distribution of the crystallographic structure of the atomic cluster aggregated along the (222) plane slightly changed under irradiation exposures. The broadening of (222) planes' peak, variations on the grain sizes (D) of the Dy_2O_3 films under irradiation exposures were calculated via well-known Scherrer's relation [20]. The calculated D values prior and after gamma irradiation exposures are shown in Table 1. It can be seen that the D values increased with increasing irradiation. Together with ionization and atomic displacement, irradiation also generates lattice vibrations which cause phonon scattering around the lattice points. It is well known that the phonon scattering may lead to the local heating. The local heating may cause the aggregation of the smaller grains into a bigger cluster [20], [21]. Thus, the rises in the D value can be attributed to the local heating generated by irradiation. The XRD analyses have depicted that no significant change has been observed under Co-60 gamma irradiation exposures. Only slight improvements of the grain size distributions have been observed.

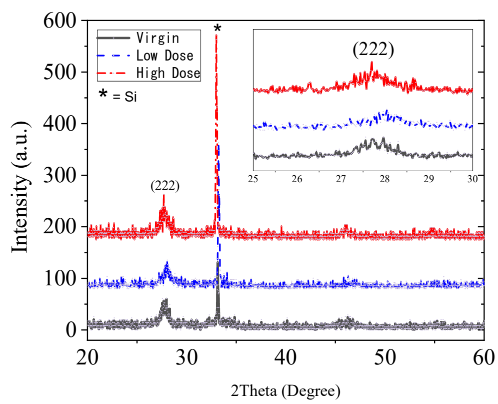

Figure 1. Irradiation-induced variations on the XRD measurements of Dy_2O_3/Si thin film

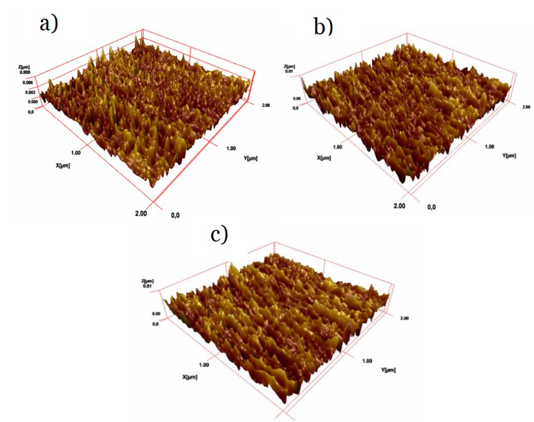

Figure 2. The AFM pictures of a- pristine, b- low dose and c- high dose exposed samples

The Atomic Force Microscopy (AFM) was used to investigate the variations in the surface morphology of the gate oxide under Co-60 gamma irradiation. The AFM images of the Dy_2O_3 films are shown in Fig. 2 (a)-(c). The morphological distribution of the irradiated films is almost the same as the virgin sample and no hillock/crack formation has been observed. This indicates that stress and strains generated by irradiation-induced defects were not too high to deteriorate the films' surface structure [22]. The root means square roughness (RMS) values of the samples were calculated using the AFM software and the calculated RMS values are listed in Table 1. Rises in the RMS values after the gamma irradiation exposures indicate the presence of the gamma irradiation-induced surface damage. The crystallization of the amorphous track causes volume expansion [23]. This crystallization, e.g., the increment of the grain size, modifies the surface morphology of the Dy_2O_3/Si thin films [19], [23].

3.2 The electrochemical characteristics of the Dy_2O_3/Si thin films prior and after irradiation exposures

The initial elemental compositions and the possible irradiation-induced changes on the surface chemistry of the Dy_2O_3/Si thin film were discussed via XPS measurement. The obtained XPS measurements were calibrated to C 1s peak at 285 eV to eliminate the possible impurity effects. The XPS spectra of the Dysprosium (Dy) and Oxygen (O) are illustrated in Fig. 3 (a) and (b), respectively. The measured XPS spectra do not have an ideal Gaussian curve shape. In other words, the measured XPS spectra consist of sub-curves which indicate that the elements have multi oxidation states in their core levels. Thus, these substrates were specified by the de-convolution of the XPS spectrum to reach accurate results. Fig. 3 (a) and (b) also represent the de-convoluted sub-peaks of Dy and O. The Dy over O atomic concentration has been listed in Table 1 as well. Abu-Zied et al. [24] have reported that the reference peak of Dy_2O_3 is located at 153.5 eV and 156.5 eV for doublet Dy 4d3/2 and 4d5/2 spin-orbit coupling core levels, respectively. The metallic Dy^0 bond is located at 150.5 eV. In addition, Pan et al. [16] have reported that the O 1s peaks at 533.0, 530.9, and 529.4 eV correspond to the bonds of Si–O, Dy–O–Si, and Dy–O, respectively. In the present study, we have seen that the doublet Dy 4d3/2 and 4d5/2 core levels are located at 152.39 eV and 156.19 eV, respectively for the virgin sample. It is known that oxygen-deficient oxide bonds are located at the binding energies (BEs) lower than fully oxidized compounds [20]. Hence, the Dy sub oxidation peaks (at 152.39 eV for 4d3/2, at 156.19 for 4d5/2) and O peak located at 529.15 may be attributed to the oxygen-deficient Dy_2O_3 bonds in the thin film structure. On the other hand, the sub-peaks of Dy having 153.75 eV and O having 528.78 eV, which are also significantly lower than stoichiometric Dy 4d5/2 and O1s states, are associated with defect-related dysprosium sub-oxide (Dy_xO_y). This intense secondary phase of the sub-dysprosium oxide may degrade the electrical performance of devices. Moreover, the last sub-oxygen peak at 530.33 eV may be associated with the interfacial oxygen bonds in non-stoichiometric $DySi_xO_y$ [16].

When the thin film was exposed to low irradiation doses, the BEs of the Dy related sub- states shifted toward lower energies. However, irradiation influences on the O related substrates were more complicated. The binding energy of the first sub-state of the O1s (states related in Dy_xO_y bonds) shifted toward lower values while the remaining sub O1s states shifted toward higher binding energy values. Irradiations cause ionization and disordered regions due to the atomic displacement. The atomic displacement may leave lattice vacancies, lodge in interstitial locations, etc. [25], [26]. The binding energy shifts to lower values are due to bonds breaking and the formation of the vacancies in the structure [20], [27]. However, the binding energy shift toward higher values may be due to either the formation of the interstitial atoms [26], or the passivation of the dangling bonds thanks to the irradiation generated local heating [19]. For the passivation process, both Dy and O related states should shift toward higher binding energies. However, in the present study, owing to Dy states shifting toward lower binding energy values, the higher binding energy shift of O1s substrates can be attributed to oxygen-related interstitial defect formation. Compared to the low-dose exposed sample, after high-dose irradiation exposures, the binding energies of both Dy and O sub-states shifted towards lower binding energies. On the other hand, after low and high dose irradiation exposures, the peak intensities of O1s states obviously enhance. These observed rises in the peak intensities may be due to the diffusion of oxygen present in the atmospheric environment into the oxide layer [19], [20]. The rise in oxygen concentration with irradiation exposure in Table 1 also supports this discussion. The XPS analyses have revealed that the binding energies basically shift toward the lower sides and these lower binding energy shifts demonstrate that bonds between Dy and O are broken by irradiation exposure. These broken bonds may act as a trap site in the structure.

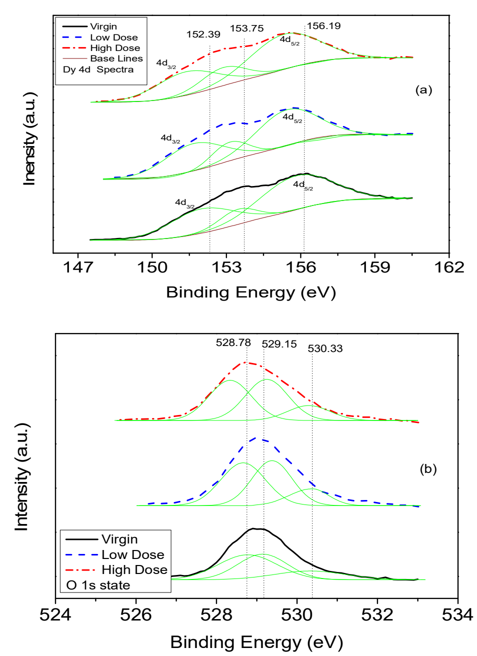

Figure 3. The XPS spectra of Dy2O3/Si thin films prior to after gamma irradiation exposures for a-) Dy4d and b-) O1s core levels

3.3 The electrical characterizations of virgin and irradiated Al/Dy_2O_3/Si/Al MOS Capacitors

The irradiation influences on the electrical characteristics of Al/Dy_2O_3/p-Si/Al MOS capacitors were investigated by analyzing capacitance-voltage (C-V) and conductance-voltage (G/ω – V) curves illustrated in Fig. 4 (a) and (b). The three distinct regimes of C–V curves, namely accumulation, depletion, and inversion, can be clearly seen for both virgin and irradiated samples. However, the capacitance curves exhibit kinks at a region between depletion and accumulation. As mentioned in XPS analysis, together with the Dy_2O_3 phase, we have observed an intense secondary phase of the dielectric layer that is called Dy_xO_y. We know that the oxygen vacancies or any defects present may affect the total dipole and polarization in the dielectric layer [28]. Hence, the observed fluctuations between depletion and accumulation regimes can be attributed to the influence of the intense parasitic Dy_xO_y phases in the structure. Similar fluctuations have also been observed in the conductance curve. Here the lower shoulder of the conductance peak may be due to the exchange of the charge carrier between the localized states in Si and the parasitic Dy_xO_y phase.

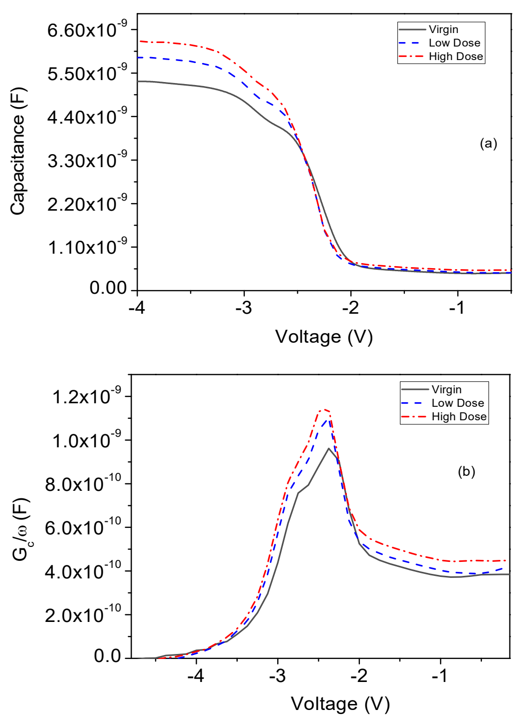

Figure 4. The electrical a-) C-V and b-) G/ω-V characteristics of virgin and irradiated Al/Dy2O3/Si/Al MOS capacitors

It can be seen from Fig. 4 (a) that the capacitance of low and high dose exposed samples is significantly increased with the increasing in the radiation dose. The possible reasons of the increase in capacitance may be explained by an increase in the interface state density (D_{it}) and may act as an additional capacitance [12], and/or the modification of the materials' dielectric specification due to the structural/electrochemical variations induced by irradiation. In the first case, the frequency dependent surface states may act like an additional capacitance which depends on whether they can follow gate bias or not [2], [29]. Hence, the D_{it} generated by irradiation may contribute the equivalent capacitance of the device which causes the rises in the capacitance curves. The D_{it} values under gamma irradiation exposures were calculated using the conductance peaks in Fig. 4 (b) via well-known Hill and Coleman technique [30]. The calculated D_{it} values and some parameters used in the calculation are given in Table 1. It is seen that D_{it} values increased with the increasing irradiation doses. The rise in D_{it} values can be attributed to the continuous creation of dangling bonds at the Dy_2O_3/Si interface. The lower binding energy shifts in some sub oxidation states in XPS analyses support this observation. On the other hand, XPS analyses have also revealed that the oxygen concentrations are enhanced with irradiation exposure and interstitial defect formation has been observed due to the oxygen diffusion. This diffused Oxygen may also increase the total polarization of the materials, i.e., the dielectric constant of the device may be enhanced by irradiation. Hence, both D_{it} generation and the improvement of the dielectric characteristics may contribute to the rises in the capacitance in different proportion.

Table 1. Irradiation-induced changes on some device characteristics.

	Grain Size (nm)	*RMS (nm)*	*[Dy]/[O]*	*G/ω_{max} (x 10^{-10} F)*	*C (x 10^{-9} F)*	*D_{it} (x 10^{12} cm^{-2} eV^{-1})*
Virgin	3.89	4.21	0.61	9.61	3.04	3.46
Low Dose	4.12	4.43	0.46	11.0	2.90	3.53
High Dose	4.61	4.62	0.44	11.4	2.91	3.70

4. Conclusion

The detailed study of Al/Dy_2O_3/p-Si/Al capacitors has been done under Co-60 gamma irradiation for the investigation of the influences on the physical, electrochemical and electrical characteristics. The crystallographic orientation is almost insensitive to the irradiation exposures, while the grain size of films slightly increases due to the local heating aggregating the smaller grains into a bigger cluster. No hillock or crack formations have been observed. This demonstrates that stress and strains generated by irradiation-induced defects were not too high to deteriorate the surface morphology. A slight increase in the RMS value can be attributed to the rises in the grain size and crystallization of the amorphous track in the film structure. On the other hand, complicated electrochemical distributions on the film structure have been observed. Both oxygen deficient Dy_2O_3 phase and an intense secondary defect-related dysprosium sub- oxide (Dy_xO_y) phase have been found for pristine samples after XPS analysis. These two chemical phase structures cause fluctuation in the capacitance and conductance curves. On the other hand, oxygen diffusion into the bulk oxide layer, vacancy, and interstitial defect formations have been observed in the electrochemical characteristics of Dy_2O_3/Si thin films after irradiation exposures. The diffused oxygen makes a new bond with dangling Dy atoms in the bulk oxide layer which increases the total dipole and dielectric characteristics of Dy_2O_3. Also, the D_{it} values increase with increasing the irradiation exposures and this may also contribute to the measured capacitance. Hence, both D_{it} generation and improvement of the dielectric characteristics contribute to the rise in the capacitance curves but possibly in different proportion. Consequently, although small modifications have been observed in the morphology and crystalline structure of the Dy_2O_3/Si thin film, irradiation significantly changes the electrochemical and dielectric characteristics of Al/Dy_2O_3/p-Si/Al capacitors.

Acknowledgements: *This work is supported by the Presidency of Turkey, Presidency of Strategy and Budget under Contract Number: 2016K121110.*

REFERENCES

1. F. B. Ergin, R. Turan, S. T. Shishiyanu, E. Yilmaz, "Effect of γ-radiation on HfO2 based MOS capacitor," *Nucl. Instrum. Methods Phys. Res.*, vol. 268, no. 9, pp. 1482 – 1485, May 2010. DOI: 10.1016/j.nimb.2010.01.027
2. S. Kaya, E. Yilmaz, "A Comprehensive Study on the Frequency-Dependent Electrical Characteristics of Sm2O3 MOS Capacitors," *IEEE Trans. Electron Devices*, vol. 62, no. 3, pp. 980 – 987, Jan. 2015. DOI: 10.1109/TED.2015.2389953
3. Y. Li et al., "Study of γ-ray irradiation influence on TiN/HfO2/Si MOS capacitor by C-V and DLTS," *Superlattice. Microst.*, vol. 120, pp. 313 – 318, Aug. 2018. DOI: 10.1016/j.spmi.2018.05.046
4. G. D. Wilk, R. M. Wallace, J. M. Anthony, "High-κ gate dielectrics: Current status and materials properties considerations," *J. Appl. Phys.*, vol. 89, no. 10, pp. 5243 – 5275, May 2001. DOI: 10.1063/1.1361065
5. S. C. Chang, S. Y. Deng, J. Y. M. Lee, "Electrical characteristics and reliability properties of metal-oxide-semiconductor field-effect transistors with Dy2O3 gate dielectric," *Appl. Phys. Lett.*, vol. 89, no. 5, pp. 10 – 13, 2006. DOI: 10.1063/1.2217708
6. A. Cherif et al., "The temperature dependence on the electrical properties of dysprosium oxide deposited on p-Si substrate," *Mater. Sci. Semicond. Process.*, vol. 29, pp. 143 – 149, Jan. 2015. DOI: 10.1016/j.mssp.2014.01.031
7. M. Leskelä, K. Kukli, M. Ritala, "Rare-earth oxide thin films for gate dielectrics in microelectronics," *J. Alloys Compd.*, vol. 418, no. 1 – 2, pp. 27 – 34, Jul. 2006. DOI: 10.1016/j.jallcom.2005.10.061
8. K. Xu et al., "Atomic Layer Deposition of Gd2O3 and Dy2O3: A Study of the ALD Characteristics and Structural and Electrical Properties," *Chem. Mater.*, vol. 24, no. 4, pp. 651 – 658, Feb. 2012. DOI: 10.1021/cm2020862
9. A. Kahraman, E. Yilmaz, "Proposal of alternative sensitive region for MOS based radiation sensors: Yb2O3," *J. Vac. Sci. Technol. A*, vol. 35, no. 6, Nov. 2017. DOI: 10.1116/1.4993545
10. A. Kahraman, E. Yilmaz, "Irradiation response of radio-frequency sputtered Al/Gd2O3/p-Si MOS capacitors," *Radiat. Phys. Chem.*, vol. 139, pp. 114 – 119, Oct. 2017. DOI: 10.1016/j.radphyschem.2017.04.003
11. A. Kahraman, E. Yilmaz, "A comprehensive study on usage of Gd2O3 dielectric in MOS based radiation sensors considering frequency dependent radiation response," *Radiat. Phys. Chem.*, vol. 152, pp. 36 – 42, Nov. 2018. DOI: 10.1016/j.radphyschem.2018.07.017
12. S. Kaya, E. Yilmaz, A. Kahraman, H. Karacali, "Frequency dependent gamma-ray irradiation response of Sm2O3 MOS capacitors," *Nucl. Instrum. Methods Phys. Res.*, vol. 358, pp. 188 – 193, Sep. 2015. DOI: 10.1016/j.nimb.2015.06.037
13. S. Abubakar, S. Kaya, H. Karacali, E. Yilmaz, "The gamma irradiation responses of yttrium oxide capacitors and first assessment usage in radiation sensors," *Sens. Actuator A-Phys.*, vol. 258, pp. 44 – 48, May 2017. DOI: 10.1016/j.sna.2017.02.022
14. F. C. Chiu, "Electrical characterization and current transportation in metal / Dy2O3 / Si structure," *J. Appl. Phys.*, vol. 102, no. 4, Aug. 2007. DOI: 10.1063/1.2767380
15. A. A. Dakhel, "Annealing effect on the dc transport mechanism in dysprosium oxide films grown on Si substrates," *J. Electron. Mater.*, vol. 35, no. 7, pp. 1547 – 1551, Jul. 2006. DOI: 10.1007/s11664-006-0147-4
16. T. M. Pan, W. T. Chang, F. C. Chiu, "Structural properties and electrical characteristics of high-*k* Dy2O3 gate dielectrics," *Appl. Surf. Sci.*, vol. 257, no. 9, pp. 3964 – 3968, Feb. 2011. DOI: 10.1016/j.apsusc.2010.11.144
17. M. Chakraverty, H. M. Kittur, "Comparison of tunnel currents through SiO2, HfO2, Ta2O5, ZrO2 and Dy2O3 dielectrics in MOS devices for ultra large scale integration using first principle calculations," in *Proc. 2013 Annu. Int. Conf. Emerg. Res. Areas (AICERA 2013)* and *2013 Int. Conf. Microelectron. Commun. Renew. Energy (ICMiCR 2013)*, Kanjirapally, India, 2013. DOI: 10.1109/AICERA-ICMiCR.2013.6575936
18. K. Lawniczak-Jablonska et al., "Surface morphology of DyxOy films grown on Si," *Appl. Surf. Sci.*, vol. 253, no. 2, pp. 639 – 645, Nov. 2006. DOI: 10.1016/j.apsusc.2005.12.150
19. S. Kaya, I. Yıldız, R. Lok, E. Yılmaz, "Co-60 gamma irradiation influences on physical, chemical and electrical characteristics of HfO2/Si thin films," *Radiat. Phys. Chem.*, vol. 150, pp. 64 – 70, Sep. 2018. DOI: 10.1016/j.radphyschem.2018.04.023
20. S. Kaya, E. Yilmaz, "Modifications of structural, chemical, and electrical characteristics of Er2O3/Si interface under Co-60 gamma irradiation," *Nucl. Instrum. Methods Phys. Res.*, vol. 418, pp. 74 – 79, Mar. 2018. DOI: 10.1016/j.nimb.2018.01.010
21. M. Ishfaq et al., "Optical and electrical characteristics of 17 keV X-rays exposed TiO2 films

and Ag/TiO2/p-Si MOS device," *Mater. Sci. Semicond. Process.*, vol. 63, pp. 107 – 114, Jun. 2017.
DOI: 10.1016/j.mssp.2017.02.009

22. L. Vlasukova et al., "Photoluminescence and enhanced chemical reactivity of amorphous SiO2 films irradiated with high fluencies of 133-MeV Xe ions," *Vacuum*, vol. 141, pp. 15 – 21, Jul. 2017.
DOI: 10.1016/j.vacuum.2017.03.007
23. K. Agashe et al., "Effect of gamma irradiation on resistive switching of Al/TiO2/n+Si ReRAM," *Nucl. Instrum. Methods Phys. Res.*, vol. 403, pp. 38 – 44, Jul. 2017.
DOI: 10.1016/j.nimb.2017.04.091
24. B. M. Abu-Zied, A. M. Asiri, "Synthesis of Dy2O3 nanoparticles via hydroxide precipitation: effect of calcination temperature," *J. Rare Earths*, vol. 32, no. 3, pp. 259 – 264, Mar. 2014.
DOI: 10.1016/S1002-0721(14)60061-2
25. B. L. Doyle, *Displacement Damage Caused by Gamma-rays and Neutrons on Au and Se*, Rep. SAND2014-19440 R, Sandia National Laboratories, Albuquerque (NM), USA, 2014.
DOI: 10.2172/1177090
26. I. G. Madiba et al., "Effects of gamma irradiations on reactive pulsed laser deposited vanadium dioxide thin films," *Appl. Surf. Sci.*, vol. 411, pp. 271 – 278, Jul. 2017.
DOI: 10.1016/j.apsusc.2017.03.131
27. Y. Jun-Feng et al., "The first-principles calculation of the effects oxygen defect on the electronic structure of SnO2," *in Proc. 2008 2nd IEEE International Nanoelectronics Conference*, Shanghai, China, 2008.
DOI: 10.1109/INEC.2008.4585569
28. B. C. Lan, J. J. Hsu, S. Y. Chen, J. S. Bow, "Forming gas annealing on physical characteristics and electrical properties of Sr0.8Bi2Ta2O9/Al 2O3/Si capacitors," *J. Appl. Phys.*, vol. 94, no. 3, pp. 1877 – 1881, Aug. 2003.
DOI: 10.1063/1.1588362
29. A. Tataroğlu et al., "Electronic and optoelectronic properties of Al/coumarin doped Pr2Se3–Tl2Se/p-Si devices," *J. Mater. Sci.: Mater. Electron.*, vol. 29, no. 15, pp. 12561 – 12572, Aug. 2018.
DOI: 10.1007/s10854-018-9372-x
30. W. A. Hill, C. C. Coleman, "A single-frequency approximation for interface-state density determination," *Solid. State. Electron.*, vol. 23, no. 9, pp. 987 – 993, Sep. 1980.
DOI: 10.1016/0038-1101(80)90064-7